

## Temperature Dependence of the Mechanical Dissipation of Gallium Bonds for Use in Gravitational Wave Detectors

Karen Haughian<sup>✉</sup>,\* Peter G. Murray<sup>✉</sup>, Stuart Hill, James Hough, Gregoire Lacaille,  
Iain W. Martin<sup>✉</sup>, Sheila Rowan, and Simon Tait<sup>✉</sup>  
SUPA, University of Glasgow, Glasgow G12 8QQ, Scotland

Riccardo Bassiri, Martin M. Fejer<sup>✉</sup>, Sudiksha Khadaka, and Ashot Markosyan  
Stanford University, Stanford, California 94305, USA

 (Received 22 November 2023; revised 27 March 2024; accepted 3 May 2024; published 5 June 2024)

The mirror suspensions in gravitational wave detectors demand low mechanical loss jointing to ensure good enough detector performance and to enable the detection of gravitational waves. Hydroxide catalysis bonds have been used in the fused silica suspensions of the GEO600, Advanced LIGO, and Advanced Virgo detectors. Future detectors may use cryogenic cooling of the mirror suspensions and this leads to a potential change of mirror material and suspension design. Other bonding techniques that could replace or be used alongside hydroxide catalysis bonding are of interest. A design that incorporates repair scenarios is highly desirable. Indeed, the mirror suspensions in KAGRA, which is made from sapphire and operated at cryogenic temperatures, have used a combination of hydroxide catalysis bonding and gallium bonding. This Letter presents the first measurements of the mechanical loss of a gallium bond measured between 10 K and 295 K. It is shown that the loss, which decreases with temperature down to the level of  $(1.8 \pm 0.3) \times 10^{-4}$  at 10 K, is comparable to that of a hydroxide catalysis bond.

DOI: [10.1103/PhysRevLett.132.231401](https://doi.org/10.1103/PhysRevLett.132.231401)

*Introduction.*—The first direct detection of gravitational waves (GW) was made in 2015 [1] and since then over 100 more signals from astrophysical sources have been detected [2] by the Advanced LIGO [3] and Advanced Virgo [4] GW detectors. These detectors are laser interferometers that monitor the separation of suspended mirrors. The mirrors and the suspension components are made from fused silica and are jointed by laser-welding fibers to attachment points on “ears,” with the ears being attached to the side of the test mass by hydroxide catalysis bonds (HCBs) [5,6]. Future detectors such as the Einstein Telescope (ET) [7] and Cosmic Explorer [8] will also be laser interferometers. However, ET and a possible future upgrade of the Cosmic Explorer will be operated at cryogenic temperatures to further reduce thermal motion of the materials and therefore increase the detector sensitivity. This temperature shift gives rise to a need to move away from fused silica in order to maintain low noise levels due to a large peak in the mechanical loss of silica at low temperatures [9]. Silicon is currently the accepted candidate material for ET [7], while sapphire is also a potential

candidate option and was the material chosen for the KAGRA [10] detector, which became operational in 2020. Extensive investigations have been carried out to show that silicon and sapphire can be jointed using HCBs [11–19]. However, so far, welding silicon in the same way as silica to make the quasimonolithic suspensions used in gravitational wave detectors remains challenging. This means we cannot simply replicate the design of the fused silica suspensions. The laser welding was crucial in allowing the bonds to be in a location where their contribution to the overall thermal noise of the suspension was not limiting and also in providing repair scenarios in the event of a suspension failure. Thus, without this welding ability, a major problem for future detectors will be the creation of suspension designs that ensure the bond thermal noise does not limit the detector performance while also incorporating vital repair scenarios. HCBs are extremely strong and reliable. However, one downside of this jointing technique is that it cannot easily be debonded after  $\sim 48$  h. It is highly desirable to investigate other jointing techniques that could either be used alongside or instead of HCBs and that would provide a strong, low loss suspension with greater potential for repair in the case of a suspension failure. The repair scenarios are increasingly important as the suspensions in a cryogenically operated detector will experience much harsher conditions than the earlier room temperature suspensions. We are thus investigating gallium bonding, which is a technique also of

---

Published by the American Physical Society under the terms of the [Creative Commons Attribution 4.0 International license](https://creativecommons.org/licenses/by/4.0/). Further distribution of this work must maintain attribution to the author(s) and the published article's title, journal citation, and DOI.

interest for other scientific applications that benefit from reversible, metallic joints [20–25]. Gallium is of interest for GW research as it has a low melting point, is nontoxic, and is not highly reactive with silicon or sapphire at the temperature range of interest for cryogenic GW detectors [26,27]. A low melting point makes it easier for good metallic bonds to be created between highly thermally conductive materials such as silicon or sapphire. This led to gallium being chosen, following initial interest in indium bonds [28,29], for compression joints in the KAGRA mirror suspensions [30]. The use of these metallic bonds opens up the possibility for different, repairable suspension designs to be investigated, potentially moving the bonds further away from the areas where lots of energy is stored in the system. Indeed the KAGRA design differs from LIGO as it utilizes fibers that are fabricated to have block shaped end points that can be hooked under attachment pieces on the sides of the mirror and bonded in compression. Another potential benefit to using these bonds over HCBs is that there is less of a concern when bonding materials of differing coefficients of thermal expansion. Although these bonds are already used in the KAGRA detector their thermal noise performance has not been characterized and thus their suitability for use in more sensitive future detectors is not known. In this Letter we show that gallium bonds have similar cryogenic loss to HCBs. This low loss, along with the ease of debonding gallium facilitating repair scenarios, means that gallium bonds are strong contenders for use in future cryogenic detectors. The low mechanical loss is a good indicator of stability, so this result is also important for wider scientific applications.

*Fabrication of gallium jointed tuning fork.*—One method, which has been previously used to measure the mechanical loss of a joint, is to resonate a sample similar to a tuning fork style with flattened prongs [19]. This method is a sensitive way of measuring bond loss and allows measurement at frequencies closer to the frequency range of interest for gravitational wave detectors than previous bond loss methods [29,31]. Here, we have constructed a tuning fork sample from three silicon tiles: one for the handle, which is used to clamp the sample; and two for the resonating prongs that are gallium bonded to opposite faces on the end of the handle. A schematic of the sample is shown in Fig. 1. These rectangular tiles were created from 4 in. diameter, 0.3 mm thick, double side polished, undoped, [100] silicon wafers with a resistivity  $> 1000 \Omega\cdot\text{cm}$  and a 80 nm silicon nitride coating on both sides. Photolithography was used to mark the rectangular geometry on the wafers, then an ion-reactive dry etching process was used to separate out the samples. The patterned wafers were then placed in a hot potassium hydroxide bath at 80 °C to etch through the wafer and release the individual samples [32]. Finally the silicon nitride layer was removed by bathing the samples in a hydrogen-fluoride bath for about 20 m. The silicon tile used for the handle was

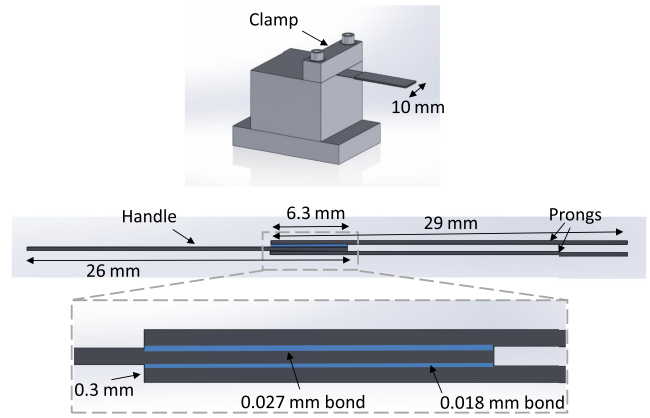


FIG. 1. Schematic diagram of the clamped gallium bonded tuning fork. The middle image shows a side view of the fork and the inset shows an enlarged view of the bonded area of the fork to show the relative thickness of the silicon and gallium layers.

$26 \times 10 \times 0.3$  mm and the two prongs were  $29 \times 10 \times 0.3$  mm. The surface flatness and roughness were characterized using a ZYGO GPI XP/D interferometer and a WYKO NT1100 optical profiling system, respectively [33,34]. The surfaces were found to have a peak-to-valley global flatness of the order of several hundred nanometers and the root mean square roughness was found to be less than 11 nm. This sets the minimum possible thickness for any bond between the two surfaces. To ensure a highly clean, hydrophilic surface was obtained prior to bonding, the samples were cleaned in Piranha solution with a 5:1 concentration of sulfuric acid to 30% hydrogen peroxide. A test tube of gallium was placed in a beaker of water on a hot plate at 80 °C in order to ensure it was in a liquid form, then a small volume of gallium, 15  $\mu\text{l}$ , was pipetted onto the clean substrate surface. An ultrasonic soldering iron was used to break up the surface oxide on the gallium to ensure good wetting of the surface and to spread the gallium over the whole bonding region. Once the whole desired region had been coated, the soldering iron was used to wipe away any excess gallium remaining on the surface to create a thin bond. The tuning fork assembly was bonded by placing the gallium coated areas together and applying pressure by hand for  $\sim 1$  m.

The mass of the individual silicon samples were measured before and after the gallium was deposited using an A&D GR-202 microbalance [35]. This information, together with the bond area and density of gallium allowed a bond thickness to be calculated. It was found that one of the gallium bonds was 0.027 mm thick and the second was 0.018 mm thick.

*Experimental setup.*—The mechanical loss was measured by monitoring the decay of the excited resonance frequencies, ( $\omega_0$ ), using the ring-down technique [36]. For this sample, the fundamental tuning fork frequency was 790 Hz at room temperature. Two other bending modes were also measured at 4.86 kHz and 13.6 kHz. To measure

the decay, the fork was mounted in a stainless steel clamp that was situated in the vacuum chamber of an IR Labs HDL-10 liquid helium cooled cryostat [37]. This allowed the mechanical loss to be measured as a function of temperature, from  $\sim 10$  to 295 K. Each resonance was excited using an electrostatic actuator that was positioned  $\sim 1$  mm below the sample and the free exponential decay of the excited resonant mode was monitored by reflecting a HeNe laser beam off the vibrating face onto a quad photodiode. By applying a fit to the amplitude ( $A$ ) of the decay of the resonant motion, the dissipation [ $\phi(\omega_0)$ ] can be calculated from

$$A(t) = A_0 e^{-\phi(\omega_0)\omega_0 t/2},$$

where  $A_0$  is the amplitude at time,  $t = 0$ . The temperature of the sample was recorded using a calibrated Lakeshore DT-670-SD temperature sensor, which was attached to the clamp directly below the sample. A Lakeshore Model 336 Cryogenic Temperature Controller was used to maintain the temperature to  $< 0.01$  K and to increase the temperature in controlled temperature steps back up to 295 K [38]. Ring-down measurements at each temperature, typically five ring-downs per temperature step, showed a variation in dissipation of  $\sim 3\%$  standard deviation on average. The experimental technique is discussed in full in [39]. The sample was resealed and recooled to check the repeatability of loss measurements. The average losses were found to be within  $\sim 20\%$  between suspensions, with the lowest losses for each resonant mode taken.

Only the elastic energy stored in the bond region “experiences” the loss of the bond and to account for this the finite element package, ANSYS, was used to model the resonant modes of the sample and determine the energy distribution. Using the calculated energy ratio, the mechanical loss of the bond can be extracted from the dissipation of the bonded sample using

$$\phi_{\text{bonded}} \simeq \frac{E_{\text{silicon}}}{E_{\text{total}}} \phi_{\text{silicon}} + \frac{E_{\text{bond}}}{E_{\text{total}}} \phi_{\text{bond}},$$

where  $\phi_{\text{bonded}}$ ,  $\phi_{\text{silicon}}$ , and  $\phi_{\text{bond}}$  are the mechanical dissipation measured for the bonded sample, estimated for the silicon substrate, and calculated for the bond respectively.  $(E_{\text{silicon}}/E_{\text{total}})$  is the ratio of energy stored in the silicon substrate to that in the whole sample, and  $(E_{\text{bond}}/E_{\text{total}})$  is the ratio of energy stored in the bond to that in the whole sample. The silicon is substantially larger than the bond, so here we can approximate  $(E_{\text{silicon}}/E_{\text{total}}) \simeq 1$ .

The fraction of energy stored in the joint region was calculated using finite element modeling over a range of temperatures, as shown in Table I, and interpolated over the measurement temperature range.

*Cryogenic mechanical loss.*—Figure 2 shows the relative motion of the resonant modes investigated of the clamped

TABLE I. Energy ratio ( $E_{\text{bond}}/E_{\text{total}}$ ), calculated using finite element modeling, over the range of temperatures studied here, for the three resonant modes.

Temperature (K)	0.78 kHz	4.86 kHz	13.64 kHz
20	0.003 06	0.003 05	0.003 06
100	0.003 08	0.003 07	0.003 08
200	0.003 11	0.003 10	0.003 12
268	0.003 10	0.003 09	0.003 11
280	0.003 16	0.003 15	0.003 17
288	0.003 22	0.003 21	0.003 23

gallium bonded tuning fork. The measured mechanical dissipation for the first resonant mode at 0.79 kHz is shown in Fig. 3. The other two resonant modes follow a similar trend. The noticeable change in the resonant frequency and in the measured loss over a very small temperature region around 288 K is likely related to the phase transition of gallium from solid to liquid [40]. To extract the mechanical loss of the joint from the measured loss of the sample, the Young’s modulus and Poisson’s ratio of all parts, and how they vary with temperature, must be known. The gallium properties were deduced from [40]. The values for shear and bulk modulus and how they vary with temperature were shifted to zero applied pressure to account for the applied pressure dependence and then fitted to allow the Young’s modulus and Poisson’s ratio to be calculated for the whole temperature range investigated here. The material property values used for the different temperature ranges are shown in Table II [40].

The substrate loss was estimated to be the sum of the predicted thermoelastic and surface losses at the resonant angular frequencies,  $\omega$ , of a 0.3 mm in thickness,  $t$ , silicon flexure. This was achieved using the equation [41]

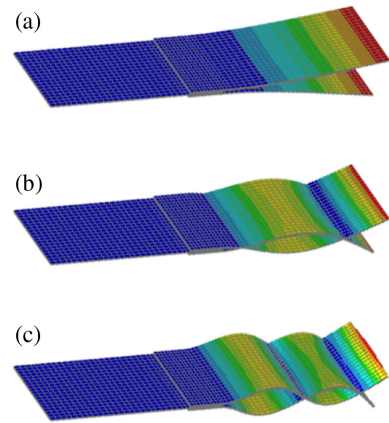


FIG. 2. Finite element representations of the (a) 0.79 kHz, (b) 4.86 kHz, and (c) 13.64 kHz resonant modes measured. The color indicates the relative magnitude of the motion, blue indicating minimal motion through to red, which indicates the maximum motion. The bending of these resonant modes is not shown to scale.

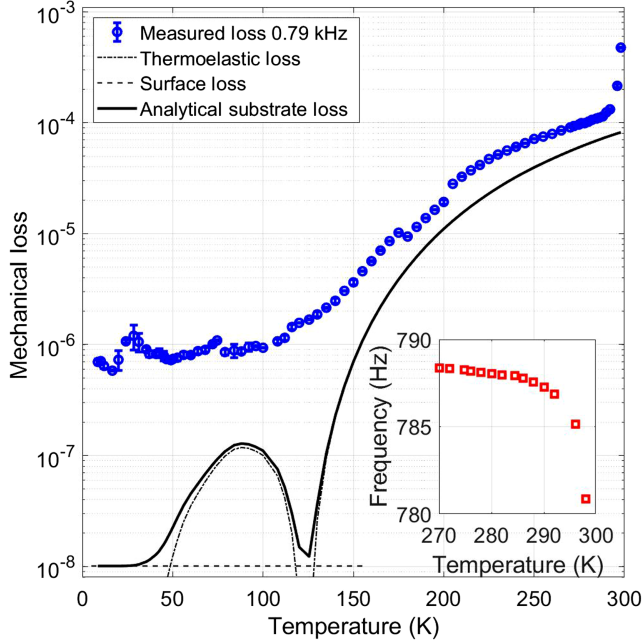


FIG. 3. Measured mechanical loss over a 10–300 K temperature range of the 0.79 kHz resonant mode of the gallium jointed tuning fork, compared to the predicted substrate loss for silicon. The inset plot shows the increasing change in resonance frequency above  $\sim 288$  K.

$$\phi_{\text{thermoelastic}} = \frac{Y\alpha^2 T}{\rho C} \frac{\omega\tau}{1 + \omega^2\tau^2},$$

where  $Y$  is the Young's modulus,  $\alpha$  is the linear thermal expansion coefficient,  $T$  is the temperature,  $\rho$  is the density,  $\kappa$  the thermal conductivity,  $C$  is the heat capacity, and  $\tau = (t^2\rho C/\pi^2\kappa)$  and [42]

$$\phi_{\text{surface}} = \alpha_s\mu \frac{S}{V},$$

where the surface loss parameter  $\alpha_s = 0.5$  pm,  $\mu$  is a geometric parameter dependent on the strain and the mode shape and was determined to be 2.94, and  $(S/V)$  is the surface-to-volume ratio of the sample [42]. This provides a good estimation of the loss of the unbonded sample at temperatures above 120 K where thermoelastic damping

TABLE II. Young's modulus and Poisson ratio of gallium over the range of temperatures studied here. Estimated from [40].

Temperature (K)	Young's modulus (GPa)	Poisson ratio
20	98.05	0.29
100	97.18	0.28
200	95.95	0.26
268	98.30	0.24
280	92.23	0.25
288	85.83	0.27

begins to become the dominant source of loss. However, as shown in Fig. 3, at lower temperatures this approximation treats the unbonded sample as being close to lossless, and thus provides a good upper limit for the bond loss.

The extracted gallium bond loss is shown in Fig. 4. It can be seen to decrease with temperature from a value of  $(1.5 \pm 0.1) \times 10^{-3}$  at 123 K down to  $(1.8 \pm 0.3) \times 10^{-4}$  at 10 K. A peak is observed in the loss at  $\approx 30$  K. This was observed on two independent cooling runs. The inset of Fig. 4 shows that, for the three resonances investigated, the temperature at which the peak occurs does not have a clear systematic frequency dependence, suggesting that it may not be caused by a thermally activated transition of the atoms. The thermoelastic loss is very low under 50 K, so it is possible that the loss peak comes from other loss mechanisms that are usually submerged by the thermoelastic loss such as phonon-phonon damping [42].

*Comparison to other jointing techniques of interest.*— Other bonding techniques that have been of interest to the gravitational wave community are hydroxide catalysis bonding and indium bonding.

Hydroxide catalysis bonding is a chemical bonding technique that involves etching the surfaces to liberate molecules that then polymerize to form strong siloxane chains between the two surfaces [43,44]. As the bond cures, dehydration occurs. This was patented by Gwo for Gravity Probe B [45] and further developed for gravitational wave detection. It has been used to successfully create strong,

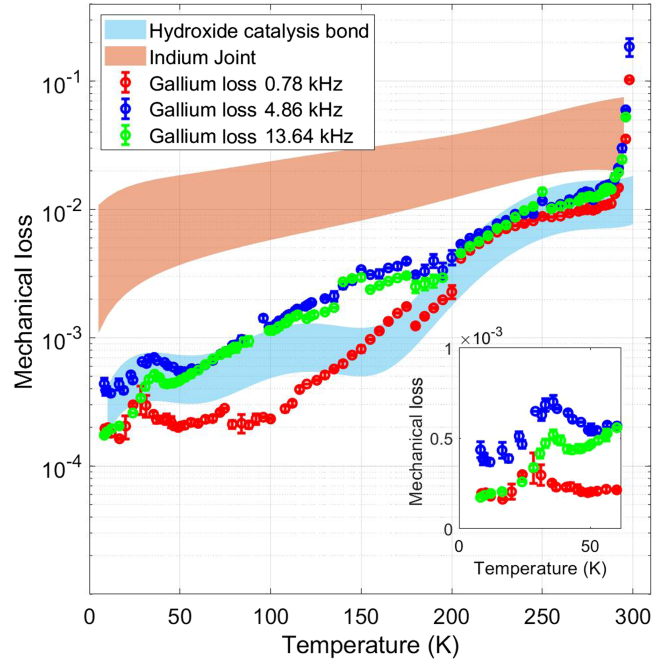


FIG. 4. Cryogenic mechanical loss of gallium calculated from the four resonant modes of the tuning fork. The range of previously reported levels of loss of hydroxide catalysis bonds (light blue) and indium (light red) are shown for comparison. The inset plot shows the small peak in loss at  $\sim 30$  K.

low loss mirror suspensions in GEO600 [46], Advanced LIGO, Advanced Virgo, and KAGRA. The loss of a hydroxide catalysis bond has been measured previously between different substrates [16,17,19,31]. The most recent paper made use of the tuning fork sample geometry. The hydroxide catalysis bond loss shown in Fig. 4 is the updated values from this work by some of the authors [47]. It can be seen in Fig. 4 that the losses measured here for gallium bonding are comparable to that of a hydroxide catalysis bond.

Indium bonding is a type of metallic bonding that has previously been investigated for use in gravitational wave detectors [28,29]. Indium has a higher melting point than gallium, making it harder to melt between high thermally conductive materials such as silicon or sapphire. Because of this, KAGRA scientists stopped attempting indium bonding for the mirror suspension and looked to the “easier to create” gallium bonding technique. Mechanical loss of indium has been measured previously, and Fig. 4 shows that gallium is not only more favorable in the practical sense of application but also due to its lower mechanical loss.

The gallium bonds studied here are of a similar thickness to the indium bonds that have been previously studied but they are substantially thicker than HCBs, which are usually tens to hundreds of nanometers in thickness. It is believed that gallium bonds could be made thinner by use of evaporation or sputtering. This would vastly reduce the thermal noise contribution to a detector and could also aid in improving the precision of the coated area size.

*Conclusion.*—The mirror suspensions for future generation gravitational wave detectors will require a change of material and design from the current fused silica, room temperature operated detectors in order to have a thermal noise level that is low enough to enable the detection of gravitational waves. Therefore, it is crucial that different jointing techniques are fully investigated in order to aid this design and allow for a suspension with the lowest possible noise and therefore the best possible sensitivity for the detector. In this Letter, we show that the mechanical loss of a gallium bond is comparable to that of a hydroxide catalysis bond, which is the current bonding technique used, and the loss decreases with temperature down to a level of  $(1.8 \pm 0.3) \times 10^{-4}$  at 10 K. This result shows that gallium is a strong candidate for use in gravitational wave detectors especially as, unlike hydroxide catalysis bonding, it can be easily debonded by elevating the temperature to the transition point at which gallium becomes liquid. Therefore, it could potentially provide repair scenarios in the case of a suspension failure, increasing the longevity of future cryogenic gravitational wave detectors and decreasing risk. Additionally, this low mechanical loss indicates good stability of the bonds, a characteristic which is of the utmost importance for many applications of reversible bonding.

We are grateful for financial support from STFC (ST/V001736/1, ST/V005634/1), from the University of Glasgow and from the Stanford Nano Fabrication Facility. R. B., M. M. F., S. K., and A. M. would like to acknowledge the support of the LSC Center for Coatings Research, jointly funded by the National Science Foundation (NSF) and the Gordon and Betty Moore Foundation (GBMF); through NSF Grants No. PHY-2011571 and PHY-2011706, and GBMF Grant No. 6793. We thank our colleagues in the LSC, Virgo, and KAGRA Collaborations and within SUPA for their interest in this work. This Letter has LIGO document no. LIGO-P2300366.

\*karen.haughian@glasgow.ac.uk

- [1] B. P. Abbott, R. Abbott, T. Abbott, M. Abernathy, F. Acernese, K. Ackley, C. Adams, T. Adams, P. Addesso, R. Adhikari *et al.*, Observation of gravitational waves from a binary black hole merger, *Phys. Rev. Lett.* **116**, 061102 (2016).
- [2] R. Abbott, T. Abbott, F. Acernese, K. Ackley, C. Adams, N. Adhikari, R. Adhikari, V. Adya, C. Affeldt, D. Agarwal *et al.*, GWTC-3: Compact binary coalescences observed by LIGO and Virgo during the second part of the third observing run, *Phys. Rev. X* **13**, 041039 (2023).
- [3] J. Aasi, B. Abbott, R. Abbott, T. Abbott, M. Abernathy, K. Ackley, C. Adams, T. Adams, P. Addesso, R. Adhikari *et al.*, Advanced LIGO, *Classical Quantum Gravity* **32**, 074001 (2015).
- [4] F. Acernese, M. Agathos, K. Agatsuma, D. Aisa, N. Allemandou, A. Allocca, J. Amarni, P. Astone, G. Balestri, G. Ballardin *et al.*, Advanced Virgo: A second-generation interferometric gravitational wave detector, *Classical Quantum Gravity* **32**, 024001 (2015).
- [5] S. Aston, M. Barton, A. Bell, N. Beveridge, B. Bland, A. Brummitt, G. Cagnoli, C. Cantley, L. Carbone, A. Cumming *et al.*, Update on quadruple suspension design for Advanced LIGO, *Classical Quantum Gravity* **29**, 235004 (2012).
- [6] D. Aisa, S. Aisa, C. Campeggi, M. Colombini, A. Conte, L. Farnesini, E. Majorana, F. Mezzani, M. Montani, L. Naticchioni *et al.*, The Advanced Virgo monolithic fused silica suspension, *Nucl. Instrum. Methods Phys. Res., Sect. A* **824**, 644 (2016).
- [7] M. Punturo, M. Abernathy, F. Acernese, B. Allen, N. Andersson, K. Arun, F. Barone, B. Barr, M. Barsuglia, M. Beker *et al.*, The third generation of gravitational wave observatories and their science reach, *Classical Quantum Gravity* **27**, 084007 (2010).
- [8] M. Evans, R. X. Adhikari, C. Afle, S. W. Ballmer, S. Biscoveanu, S. Borhanian, D. A. Brown, Y. Chen, R. Eisenstein, A. Gruson *et al.*, A horizon study for Cosmic Explorer: Science, observatories, and community, [arXiv:2109.09882](https://arxiv.org/abs/2109.09882).
- [9] V. Mitrofanov, V. Braginsky, and V. Panov, *Systems with Small Dissipation* (University of Chicago Press, 1985).
- [10] T. Akutsu, M. Ando, K. Arai, Y. Arai, S. Araki, A. Araya, N. Aritomi, Y. Aso, S. Bae, Y. Bae *et al.*, Overview of kagra: Detector design and construction history, *Prog. Theor. Exp. Phys.* **2021**, 05A101 (2021).

- [11] A. Van Veggel, J. Scott, D. Skinner, B. Bezensek, W. Cunningham, J. Hough, I. Martin, P. Murray, S. Reid, and S. Rowan, Strength testing and SEM imaging of hydroxide-catalysis bonds between silicon, *Classical Quantum Gravity* **26**, 175007 (2009).
- [12] A. Dari, F. Travasso, H. Vocca, and L. Gamaitoni, Breaking strength tests on silicon and sapphire bondings for gravitational wave detectors, *Classical Quantum Gravity* **27**, 045010 (2010).
- [13] N. Beveridge, A. Van Veggel, M. Hendry, P. Murray, R. Montgomery, E. Jesse, J. Scott, R. Bezensek, L. Cunningham, J. Hough *et al.*, Low-temperature strength tests and SEM imaging of hydroxide catalysis bonds in silicon, *Classical Quantum Gravity* **28**, 085014 (2011).
- [14] N. Beveridge, A. Van Veggel, L. Cunningham, J. Hough, I. Martin, R. Nawrodt, S. Reid, and S. Rowan, Dependence of cryogenic strength of hydroxide catalysis bonded silicon on type of surface oxide, *Classical Quantum Gravity* **30**, 025003 (2012).
- [15] R. Douglas, A. Van Veggel, L. Cunningham, K. Haughian, J. Hough, and S. Rowan, Cryogenic and room temperature strength of sapphire jointed by hydroxide-catalysis bonding, *Classical Quantum Gravity* **31**, 045001 (2014).
- [16] K. Haughian, R. Douglas, A. Van Veggel, J. Hough, A. Khalaidovski, S. Rowan, T. Suzuki, and K. Yamamoto, The effect of crystal orientation on the cryogenic strength of hydroxide catalysis bonded sapphire, *Classical Quantum Gravity* **32**, 075013 (2015).
- [17] K. Haughian, D. Chen, L. Cunningham, G. Hofmann, J. Hough, P.G. Murray, R. Nawrodt, S. Rowan, A. Van Veggel, and K. Yamamoto, Mechanical loss of a hydroxide catalysis bond between sapphire substrates and its effect on the sensitivity of future gravitational wave detectors, *Phys. Rev. D* **94**, 082003 (2016).
- [18] M. Phelps, M. M. Reid, R. Douglas, A.-M. van Veggel, V. Mangano, K. Haughian, A. Jongschaap, M. Kelly, J. Hough, and S. Rowan, Strength of hydroxide catalysis bonds between sapphire, silicon, and fused silica as a function of time, *Phys. Rev. D* **98**, 122003 (2018).
- [19] L. Prokhorov, D. Koptsov, M. Matushechkina, V. Mitrofanov, K. Haughian, J. Hough, S. Rowan, A. van Veggel, P. Murray, G. Hammond *et al.*, Upper limits on the mechanical loss of silicate bonds in a silicon tuning fork oscillator, *Phys. Lett. A* **382**, 2186 (2018), special Issue in memory of Professor V.B. Braginsky.
- [20] Z. Ye, G.Z. Lum, S. Song, S. Rich, and M. Sitti, Phase change of gallium enables highly reversible and switchable adhesion., *Adv. Mater.* **28**, 5088 (2016).
- [21] E. Diller, N. Zhang, and M. Sitti, Modular micro-robotic assembly through magnetic actuation and thermal bonding, *J. Micro-Bio Robot.* **8**, 121 (2013).
- [22] Y. Mengüç, S. Y. Yang, S. Kim, J. A. Rogers, and M. Sitti, Gecko-inspired controllable adhesive structures applied to micromanipulation, *Adv. Funct. Mater.* **22**, 1246 (2012).
- [23] S. Kim, J. Wu, A. Carlson, S. H. Jin, A. Kovalsky, P. Glass, Z. Liu, N. Ahmed, S.L. Elgan, W. Chen *et al.*, Micro-structured elastomeric surfaces with reversible adhesion and examples of their use in deterministic assembly by transfer printing, *Proc. Natl. Acad. Sci. U.S.A.* **107**, 17095 (2010).
- [24] V. Sariola and M. Sitti, Mechanically switchable elastomeric microfibrillar adhesive surfaces for transfer printing, *Adv. Mater. Interfaces* **1**, 1300159 (2014).
- [25] H. Wu, V. Sariola, C. Zhu, J. Zhao, M. Sitti, and C. J. Bettinger, Transfer printing of metallic microstructures on adhesion-promoting hydrogel substrates, *Adv. Mater.* **27**, 3398 (2015).
- [26] P.H. Keck and J. Broder, The solubility of silicon and germanium in gallium and indium, *Phys. Rev.* **90**, 521 (1953).
- [27] V. Apostolopoulos, L. Hickey, D. Sager, and J. Wilkinson, Diffusion of gallium in sapphire, *J. Eur. Ceram. Soc.* **26**, 2695 (2006).
- [28] P. G. Murray, I. W. Martin, L. Cunningham, K. Craig, G. D. Hammond, G. Hofmann, J. Hough, R. Nawrodt, D. Reifert, and S. Rowan, Low-temperature mechanical dissipation of thermally evaporated indium film for use in interferometric gravitational wave detectors, *Classical Quantum Gravity* **32**, 115014 (2015).
- [29] G. Hofmann, D. Chen, G. Bergmann, G. Hammond, M. Hanke, K. Haughian, D. Heiwert, J. Hough, A. Khalaidovski, J. Komma *et al.*, Indium joints for cryogenic gravitational wave detectors, *Classical Quantum Gravity* **32**, 245013 (2015).
- [30] S. Miyoki, Current status of KAGRA, in *Ground-based and Airborne Telescopes VIII*, International Society for Optics and Photonics Vol. 11445 (SPIE, 2020), p. 114450Z, 10.1117/12.2560824.
- [31] L. Cunningham, P. Murray, A. Cumming, E. Elliffe, G. Hammond, K. Haughian, J. Hough, M. Hendry, R. Jones, I. Martin *et al.*, Re-evaluation of the mechanical loss factor of hydroxide-catalysis bonds and its significance for the next generation of gravitational wave detectors, *Phys. Lett. A* **374**, 3993 (2010).
- [32] T. H. Metcalf, X. Liu, and M. R. Abernathy, Improving the mechanical quality factor of ultra-low-loss silicon resonators, *J. Appl. Phys.* **123** (2018).
- [33] Zygo website, <http://www.zygo.com>, accessed: 2023-05-12.
- [34] Veeco wyko nt1100 optical profiler, <https://anff-q.org.au/wp-content/uploads/2016/07/3D-optical-profiler-Veeco-Wyko-NT1100.pdf>, accessed: 2023-05-12.
- [35] A&d website, [www.aandd.jp](http://www.aandd.jp), accessed: 2023-10-2.
- [36] B. S. Berry and W. C. Pritchett, Vibrating reed internal friction apparatus for films and foils, *IBM J. Res. Dev.* **19**, 334 (1975).
- [37] Ir labs liquid cryogen cryostat, <https://www.irlabs.com/products/cryostats/liquid-cryogen-dewars/>, accessed: 2023-05-12.
- [38] Lakeshore temperature controller model 336, <https://www.lakeshore.com/products/categories/overview/temperature-products/cryogenic-temperature-controllers/model-336-cryogenic-temperature-controller>, accessed: 2023-05-12.
- [39] I. W. Martin, R. Bassiri, R. Nawrodt, M. Fejer, A. Gretarsson, E. Gustafson, G. Harry, J. Hough, I. MacLaren, S. Penn *et al.*, Effect of heat treatment on mechanical dissipation in Ta<sub>2</sub>O<sub>5</sub> coatings, *Classical Quantum Gravity* **27**, 225020 (2010).
- [40] A. Lyapin, E. Gromnitskaya, O. Yagafarov, O. Stal'gorova, and V. Brazhkin, Elastic properties of crystalline and liquid gallium at high pressures, *J. Exp. Theor. Phys.* **107**, 818 (2008).

- [41] C. Zener, Internal friction in solids II. General theory of thermoelastic internal friction, *Phys. Rev.* **53**, 90 (1938).
- [42] R. Nawrodt, C. Schwarz, S. Kroker, I. W. Martin, R. Bassiri, F. Brückner, L. Cunningham, G. D. Hammond, D. Heinert, J. Hough, T. Käsebier, E.-B. Kley, R. Neubert, S. Reid, S. Rowan, P. Seidel, and A. Tünnermann, Investigation of mechanical losses of thin silicon flexures at low temperatures, *Classical Quantum Gravity* **30**, 115008 (2013).
- [43] D. Gwo, Ultra precision and reliable bonding method, US patent No. 6284085B1 (4th September 2001).
- [44] D. Gwo, Hydroxide-catalyzed bonding, US patent No. 6548176B1 (15th April 2003).
- [45] D. Gwo, Two unique aspects of gravity probe-b star-tracking space telescope:(1) Focal-plane roof-edge diffraction and (2) Fused-quartz bonding for 2.5-Kelvin applications, in *Space Telescopes and Instruments V*, International Society for Optics and Photonics Vol. 3356 (SPIE, 1998), pp. 892–903.
- [46] K. L. Dooley *et al.*, Geo 600 and the geo-hf upgrade program: successes and challenges, *Classical Quantum Gravity* **33**, 075009 (2016).
- [47] A. A. van Veggel, on behalf of the IGR, Cryogenic suspensions for future gravitational wave detectors (2018), Talk at GWADW. LIGO document number LIGO G1800845.